



Design of a reconfigurable front-end for a multistandard receiver for the frequency range of 800 MHz to 2.5 GHz

G. Zare Fatin¹ | Z.D. Koozehkanani² | Ali Fotowat-Ahmady³ | Jafar Sobhi² | Ronan Farrell⁴

¹Department of Electrical Engineering, University of Mohaghegh Ardabili, Ardabil 56199-11367, Iran

²Department of Electrical Engineering, University of Tabriz, Tabriz, Iran

³Department of Electrical Engineering, Sharif University of Technology, Tehran, Iran

⁴Department of Electronic Engineering, National University of Ireland, Maynooth, Ireland

Correspondence

G. Zare Fatin, Department of Electrical Engineering, University of Mohaghegh Ardabili, Ardabil 56199-11367, Iran.
Email: zare@uma.ac.ir

Summary

In this paper, a reconfigurable receiver front-end for the frequency range of 800 MHz to 2.5 GHz is presented. The radio frequency front-end is realized in wideband form with reconfigurable baseband filter. The proposed front-end targets the GSM, WLAN, WCDMA, and GPS standards residing in the aimed frequency range. The necessary specifications for each individual standard have been revisited and recalculated. The interaction of the different standards and their interoperability has been thoroughly investigated and extra specifications derived for the multistandard receiver. The multistandard receiver has been designed, layouted, and simulated in RFCMOS 0.18- μm process.

KEYWORDS

multistandard, out-of-band linearity, RF front-end, wideband

1 | INTRODUCTION

The proliferation of wireless communication devices and different communication standards and protocols, besides the evolution of the former standards, entails the use of a multistandard transceiver. The simple solution for multistandard realization is to implement parallel transceivers; obviously, this is not an efficient design regarding the area and power consumption.^{1,2} The counterpoint of this realization is the software-defined radio shown in Figure 1 with utmost flexibility and efficient realization. But, at the moment and for near future, direct digitization of the radio frequency (RF) signal at antenna seems not feasible. This would need a huge effort and if realizable enormous power consumption in the data conversion blocks.³

A midpoint between these two extreme realization is a reconfigurable front-end which processes the signal before the data conversion stage and digital signal processing blocks.⁴⁻⁸ A general representation of this front-end for a receiver is shown in Figure 2. This front-end comprises reconfigurable blocks that can be changed based on the targeted standard. The demonstrated front-end is a general representation which can be implemented in different ways based on the desired specifications and also targeted standards. Most reconfigurable RF front-ends⁹⁻¹¹ are using narrow band blocks like low-noise amplifiers (LNAs)¹² and mixers which can be tuned to receive the desired frequency band. This tuning can be done in the input matching network or the load of the block. Some realizations¹³ also use parallel blocks, which can be selected for the desired reception or transmission band. The narrow band blocks can mitigate the linearity and out-of-band intermodulation issues that are very crucial in the multistandard realization. However, they are not very efficient in the area and block reusability.

In this paper, a wideband RF front-end is chosen over the narrow band implementation, which favors the block reusability but demands the higher in-band and out of band linearity from the front-end.

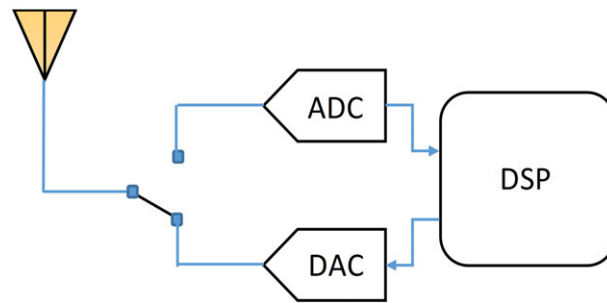


FIGURE 1 An software-defined radio [Colour figure can be viewed at wileyonlinelibrary.com]

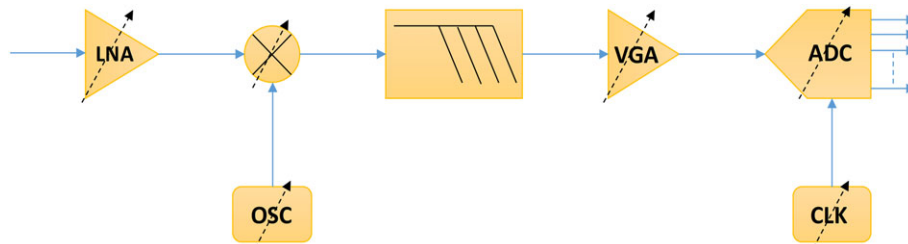


FIGURE 2 A reconfigurable radio receiver [Colour figure can be viewed at wileyonlinelibrary.com]

The proposed wideband front-end is using a current-mode architecture to increase the linearity. The RF signal is processed in current mode and then is converted back to voltage after the baseband filtering. The building blocks of the front-end have been designed to achieve high linearity. The low-noise transconductance amplifier (LNTA) is the first block facing the RF signal. This LNTA converts the RF signal to current mode, which is then processed by passive mixer.

In this work, an extensive analysis of the system level requirements of the different communication standards has been performed. These are mostly the standards covered by the proposed receiver. These calculations have been carried out for a single standard as well as in multistandard scenario, which poses higher requirements on the receiver. The second- and IMD3 that arose due to simultaneous operation of the different aimed standards were also investigated, and their possible interference with the receive bands of the other standards was evaluated. In this case, the out-of-band linearity requirements of the receiver were discovered, which must be fulfilled in addition to the in-band linearity requirements.

The system level requirements of the different blocks inside the front-end were studied, and their gain, noise and linearity requirements were defined. The proposed transimpedance amplifier (TIA) in the front-end chain is used to convert the signal back to the voltage mode. The proposed TIA has filtering function embedded inside which gives the front-end architecture extra degree of freedom and helps to relax the baseband filtering requirements.

The rest of the paper is organized as follows: In section 2, the overall architecture of the front-end is presented, and section 3 presents the requirements of the different targeted standards. Section 4 discusses the interoperability requirements of the front-end from the linearity viewpoint, and section 5 describes the receiver implementations and individual block requirements. In this section, the circuit level design of the different blocks is also explained. Section 6 presents the chip layout and simulation results; finally, some conclusions are drawn in section 7.

2 | ARCHITECTURE OF THE FRONT-END AND TARGETED STANDARDS

In realization of a single-mode receiver, sensitivity, selectivity, and maximum signal level are among the main specifications that should be considered and evaluated. In the transmitter side, output power level and emission mask are the most important specifications. However, in multimode transceivers, other extra specifications are also needed to be taken into account. These are (1) blocking effect of the transmitter, which belongs to another standard realized on the same chip; (2) noise created by tail of the other transmitter; (3) intermodulation effect of the other transmitter

and a blocker; (4) coupling effect of the local oscillator (LO) signal coming from the other standard working on the same chip.

A multimode receiver can be realized in two ways, according to the concurrency of the reception: (a) In the first state, simultaneous communication with two different standards at the same time is possible. (b) In the second case, the receiver is configured to receive just one selected standard at a time. In a multistandard receiver, dealing with interferer signals is very challenging. This becomes more difficult when the receiver is designed for instance to receive two different standards simultaneously. However, even in a reconfigurable receiver which is designed to receive just one standard at a time, there is still possibility of receiving interfering signals; this is due to the time domain behavior of the standards.

With this brief explanation of the challenges that a multistandard realization faces, it can be surmised that a multistandard receiver will have tougher and broad range of specifications in comparison with a single mode realization.

In Figure 3, the overall architecture of the proposed front-end is shown. A wideband LNA is preceded by several Surface Acoustic Wave (SAW) filters, which filter out the signal from targeted standards. The LNA is followed by a wideband mixer. The LNA and mixer will be further explained in section 3. The tunable base band filter comes after mixer and can be reconfigured to desired bandwidth based on the received standard. In this paper, only the I path of the sketched receiver has been realized; in fact, the Q path is the replication of the I path. The mixer is derived from an ideal source; the design of the VCO for the proposed front-end is described in another article.¹⁴

In this paper, the targeted standards include the GSM900/1800, W-CDMA2100, WLANb/g, and Global Positioning System (GPS). The utilization of the isolated front-ends for implementation of these standards has been reported in several articles. The wideband receiver can be used as a multistandard receiver inside a software-defined radio. However, a wideband receiver should possess a high linearity to be able to use inside a multistandard receiver. The current-mode receiver can achieve notable linearity performance, but it suffers from high noise figure (NF) and low gain value. However, in this realization, the only standard with very strict NF specification is GPS, and other standards demand moderate NF value.

3 | REQUIREMENTS OF THE STANDARDS AND THEIR INTEROPERABILITY

3.1 | GSM850/900/DCS1800/PCS1900

Except DCS1800, other GSM revisions require sensitivity level of -104 dBm; the sensitivity value for DCS is equal to -102 dBm.¹⁵ GSM standard should achieve 2% bit error rate (BER) in this reference sensitivity level. This BER is equivalent to E_b/N_0 of about 4.8 dB. The Bit rate of the different revisions of the GSM standard is equal to 270 kbps and with channel spacing of 200 kHz, then the minimum required signal-to-noise ratio (SNR) is equal to 6.2 dB; usually, with some safety margin 7 dB of minimum SNR is approved.

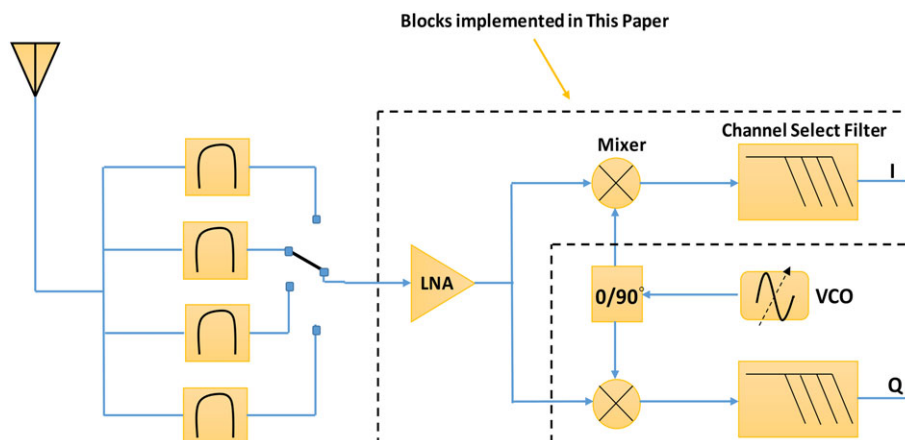


FIGURE 3 The architecture of the proposed front-end [Colour figure can be viewed at wileyonlinelibrary.com]

3.1.1 | Noise figure

The NF value for the GSM receiver can be calculated from the sensitivity requirement. As mentioned above, to get the necessary sensitivity, a minimum SNR value of 7 dB is required. For DCS1800, the power of the noise at antenna should be below -109 dBm; this is equal to -111 dBm for other revisions of the GSM. The noise of the source resistor at 290°K and for the bandwidth of 200 kHz is equal to -121 dBm. Therefore, the NF of the DCS receiver at antenna should be less than 12 dB. For other revisions of the GSM standard, the NF value should be less than 10 dB. Assuming about 4 dB of loss for RF radio module including the channel select filter (CSF), switches, and PCB lines, the NF requirement for DCS1800 is 8 dB and for other revisions of the GSM is equal to 6 dB.

3.1.2 | IIP3

Because PCS1900 and GSM800/900 require higher IIP3 in comparison with DCS1800, then just IIP3 of these standards is evaluated. Based on the standard definition,¹⁵ the signal level that is 3 dB above reference sensitivity should be received with desirable BER. This is achieved while a continuous static sinusoidal signal with power level of -43 dBm and with 800-kHz space from the main signal and another GMSK modulated signal with power level of -43 dBm and 1.6-MHz space from the main signal exists at the input of the receiver. The intermodulation of these two sinusoidal and GMSK signals should be below -112 dBm. The 4-dB reduction in desired signal power level that was accounted for is due to RF module attenuation. This will also be deducted from the interfering signals power. Then, the IIP3 of the receiver is calculated as

$$\text{IIP3} = \frac{3P_{\text{int}} - P_{\text{IMDsin}}}{2} \quad (1)$$

In this equation, P_{int} is the power of interfering signal and P_{IMDsin} is the acceptable intermodulation level at the input of the receiver. Therefore, the required IIP3 for the receiver is equal to -14.5 dBm.

3.1.3 | Image rejection ratio

According to the standard¹⁵ specifications, the reference sensitivity level should be achieved in the presence of the co-channel and adjacent channel interferers. The co-channel interferer is generated by a distant mobile station that is transmitted in the same frequency. The adjacent channels are used by other people in the same cell.

The image rejection ratio is calculated when the co-channel interferer is 9 dB below the signal, the first adjacent signal is also 9 dB higher than the desired signal, and the second adjacent signal is 41 dB higher than the desired signal. The requirements for interference signals are evaluated when the desired signal is 20 dB higher than reference sensitivity level along with a continuous GSM modulated interferer signal. Therefore, receiver noise is not important in this state.

The worst-case state is when the desired signal and interferer are located opposite of each other in two different sides of the LO. Then, the attenuated interferer signal is folded onto the desired signal after down conversion.

For a low-IF GSM receiver with IF equal to 100 kHz, and channel spacing of 200 kHz and with interference scenario explained above, having infinite image rejection ratio, achievable SNR for the signal is about 9 dB. Because the adjacent interferer is folded back onto the desired signal channel, then it should be attenuated as low as the amplitude of co-channel interferer. Therefore, the required image rejection (IM) for the receiver is about 18 dB. This value of IM is more than necessary, because the targeted SNR is about 7 dB.

The requirement of the IM for the interferer signal at 400 kHz away from the desired signal is higher. After down conversion, this interferer perches at 300 kHz, but the tail of this interferer signal at 200 kHz away from the signal is also folded back onto the desired signal; therefore, it would be necessary to attenuate this interferer to the level of the adjacent signal at 200 kHz distance. Therefore, the required IM in this case is about 32 dB.

3.1.4 | IIP2

The IIP2 requirement for a low or zero-IF GSM receiver is high and challenging. Although the GMSK signal with constant envelope does not generate the wideband second-order intermodulation, however, in the standard, there is a specification for AM (amplitude modulation) rejection. This has been mentioned to prevent receiver desensitization due to

another GMSK jammer, which is generated by on/off switching in the other transmitting carrier. According to the standard, a desired signal with the power level of -99 dBm should be demodulated in the presence of an AM modulated interferer with the power level of -31 dBm. Then, the required IIP2 is

$$\text{IIP2} > 2P_{\text{AM}} - \text{noise floor} \quad (2)$$

where in this equation P_{AM} is the power of the AM modulated interferer. This gives an IIP2 requirement higher than $+49$ dBm that is very challenging to achieve. For instance, this would be translated to IIP2 of about 65 to 70 dBm for the mixer with 16 to 18 dB gain in the LNA.

3.2 | WCDMA2100

3.2.1 | Noise figure

According to the 3GPP definition, the reference sensitivity is the minimum power level detectable by receiver at the antenna port when the BER is less than 10^{-3} . This defines the NF requirement of the receiver. Considering the modulation and coding scheme used in the transmitter and the power of the received signal before despreading, which is equal to -107 dBm, then the tolerable interference level after despreading is about -99 dBm. With this tolerable interference level and considering the thermal noise of the source resistance at 290°K for the bandwidth of 3.84 MHz, then the required NF of the receiver at antenna is equal to 9 dB. Assuming that duplexer has about 2 dB of loss, therefore, the required NF value is about 7 dB at the input of the receiver.

3.2.2 | In-band IIP3

For the intermodulation test, two different types of interferer signals are used. One of them is the continuous-wave signal, and the other one is a WCDMA modulated. The power level of these signals is -46 dBm, the continuous-wave signal is 10 MHz away, while the modulated signal lies 20 MHz away from the desired signal. The desired signal level in this case is -104 dBm. After separation of the noise plus intermodulation and referring them to their generating source,¹⁶ the acceptable intermodulation level at the input is -104.3 dBm. Therefore, required IIP3 value is about -16.9 dBm.

3.2.3 | Out-of-band IIP3

Leakage of the transmitter to the receiver in the presence of a continuous-wave interferer signal creates an intermodulation tone in the signal band. The transmitter leakage is 135 MHz away from the desired signal; the power level of this leakage signal is about -30 dBm.¹⁷ The continuous-wave interferer signal power is about -40 dBm and is 67.5 MHz away from the main signal. The desired signal power in this case is 3 dB higher than reference sensitivity when accompanied with interfering signals; the noise power level is -99 dBm, then required IIP3 is calculated as

$$\text{IIP3}_{\text{out-of-band}} = \frac{T_{\text{leak}}[\text{dBm}] + 2P_{\text{cw}} - (P_{\text{IMD3in}}[\text{dBm}] - \text{IL}(\text{dB}))}{2} \quad (3)$$

which is equal to -4.5 dBm. In this equation, T_{leak} is the leakage of the transmitter to the receiver, P_{cw} is the power of the continuous wave interferer signal, and IL accounts for the in-band loss of duplexer, which, in this case, is assumed to be equal to 2 dB.

3.2.4 | IIP2

Due to second-order nonlinearity in the receiver, the leakage signal of the transmitter can generate low-frequency intermodulation products that can be transferred to the baseband frequencies by phase noise of the LO. The leakage signal of the transmitter can be as large as -24.5 dBm, which is stronger than blocker signal defined in the standard.¹⁸ In the reference sensitivity evaluation, the NF value should be less than 9 dB to account for the additional second-order distortion generated by the transmitter leakage. Therefore, the IIP2 can be written as

$$IIP2 = 2T_{\text{leak}} - 10 \log \left(10^{\frac{-99.2 \text{ dBm}}{10}} - 10^{\frac{-108.2 \text{ dBm} + \text{NF}}{10}} \right) + \text{CorrFactor} \quad (4)$$

The term inside the parentheses represents the intermodulation distortion referred to the input with NF value of 9 dB. The correction factor (CorrFactor) here stands for the difference between intermodulation product generated by a modulated signal in comparison with the one that is generated by two independent tones. In this case, this correction factor is considered equal to -6 dB. For example, for NF value of 8 dB, the required IIP2 is $+52$ dBm. In this calculation, the reciprocal mixing between the leakage signal of the transmitter and phase noise of the LO should also be considered. The phase noise of the LO at frequency offset of 135 MHz is important, which should be less than -150 dBc/Hz.¹⁶ This value of phase noise can be achieved with VCOs that are realized in CMOS process and with reasonable current consumption and common quality factor for the passive elements.

3.3 | WLAN b/g

The WLANg standard requires a sensitivity level higher than -83 dBm at data rate of 6 Mbps and a sensitivity better than -65 dBm at data rate of 54 Mbps. In higher data rates, the required sensitivity is decreased. On the other hand, a typical practical OFDM system needs 20 dB of SNR to achieve packet error rate less than 10%. Therefore, the necessary SNR for data rate of 6 Mbps is equal to 5 dB.¹⁹

With minimum SNR and sensitivity in hand, the NF value can be calculated according to

$$\text{NF} = \text{sensitivity} - kT - 10 \log \text{BW} - \text{SNR} \quad (5)$$

In Eq. 5, the BW is equal to the modulated signal bandwidth. For data rate of 6 Mbps in WLANg, the minimum necessary SNR is equal to 5 dB and the channel BW is 16.3 MHz. Therefore, the NF value is equal to 13.8 dB. This requirement for NF value is for the entire system and includes the front-end module. Assuming about 3 dB of loss for this module, the NF requirement of the receiver is equal to 10.8 dB.

The Institute of Electrical and Electronics Engineers (IEEE) 802.11 standard does not have specification for the intermodulation test. However, the linearity of the receiver can be expressed in the 1-dB compression point. This standard just states the power of the adjacent channel, but in real-world application, the nonadjacent channel or a blocker also exists. In this case, the desired signal with power level of a -70 dBm should be received in the presence of an adjacent modulated signal with power of -35 dBm or a continuous-wave interferer signal with power level of -30 dBm. This interfering signal defines the 1-dB compression point; then assuming 4 dB of safety margin the 1-dB compression point is equal to -26 dBm. In 802.11b, the largest signal power is about -10 dBm. In this state, there is a stringent specification for data rate of 2 Mbps. This requires that a signal with power level of -4 dBm should be received and demodulated. Therefore, the 1-dB compression point of the receiver in the low gain mode is about 0 dBm. In 802.11g, the maximum received signal power according to the standard is -20 dBm that will result in 1-dB compression point of -10 dBm that should be achieved in low gain mode.

3.4 | Global Positioning System

In the L1 band of the GPS receiver, the power of the C/A coded (civilian application) signal is -130 dBm, whereas power of the noise in the L1 bandwidth (20 MHz) is about -101 dBm. The biggest part of the C/A power is located in a 2-MHz bandwidth that is named as main lobe. If the bandwidth is limited to this 2-MHz value, then 10-dB reduction in the noise level is achieved which is now about -110 dBm. If only the main lobe of the signal is considered, then demodulated GPS signal (50 b/s) will be negligibly corrupted. Although the bandwidth reduction from 20 to 2 MHz reduces the noise power; however, the SNR of the received signal is still about -19 dB.

The negative SNR in this case can be recovered because the correlation of the received signal with the correct satellite code will increase the signal power out of the noise. This correlation according to 6 can generate the gain value of about 43 dB for the C/A coded signal.

$$G_p = 10 \log_{10} \left(\frac{T_d}{T_c} \right) \approx 10 \log_{10} \left(\frac{20\text{ms}}{1\mu\text{s}} \right) = 43 \text{ dB} \quad (6)$$

In this equation, T_d is the navigation data bit period and T_c is the code bit period. If the antenna is at 290°K and the receiver is noiseless, then SNR after correlation process is about 24 dB. Nevertheless, designing a noiseless receiver is not possible and the NF of the practical receiver will be subtracted from the processing gain. Therefore, designing a low-noise receiver is necessary to receive and process a GPS signal.

The requirements of a GPS receiver are summarized in Table 1. There is no specification for the IIP3, and only 1-dB compression point is given. The receiver NF should be kept below 6 dB.

In low-cost applications, this feature of the C/A-coded signal, which has a main lobe with small bandwidth inside a larger channel, can be very beneficial. For instance, for a low-IF receiver and with IF of 2 MHz, the image frequency will reside inside the GPS frequency band. Therefore, the power of the image signal is comparable with the main signal and an image rejection of about 10 dB will be adequate and can be achieved with typical matching techniques. Besides, the frequency range of 3 to 7 MHz can be used for the filter transition band, which can relax the filter order and reduce the filter power consumption for the targeted dynamic range. This makes the low-IF architecture favorable for the GPS receiver.

4 | THE INTERFERENCE DUE TO MULTISTANDARD OPERATION

Although in this implementation simultaneous reception and transmission of different standards are not considered, due to time domain characteristic of the targeted standards, it is possible that a receiver would be enabled at the same time with another transmitter. The surmised interferences are investigated based on frequency band of the targeted transmitters and receivers. The investigation was performed by using codes that are written in EXCEL spreadsheet and C programming language. In this investigation, the IEEE 802.11a and Bluetooth (BT) standards are also included to resemble a more realistic environment. Even if these standards do not reside on the same die, they can exist in the nearby chips working on the same board. The results of these investigations are shown in Tables 2 and 3. Table 2 shows the summary of possible third-order intermodulation (IMD3) interferences between the evaluated standards. As shown in this table, the intermodulation of DCS1800, PCS1900, and WCDMA2100 with 802.11a is generating IMD3 products on the GPS signal. In addition, the third-order intermodulation of DCS1800 with 802.11a will create an interference in the BT band. The IMD3 of BT and 802.11a is also creating an interferer in the GSM850/900 band.

As shown in Table 3, second-order intermodulation distortion between GSM850/900 and 802.11b/g or BT will create an interference on the GPS signal. The GPS receiver needs a high sensitivity and having an interferer in the band will reduce its ability to receive the signal levels that are below the thermal noise floor. In this investigation, it was assumed that only one standard from a family is active at a specific time slot. For example, only one standard from different generations (2G, 2.5G, and 3G) has been selected and only one standard from different versions of 802.11 family is chosen.

The anticipated interferences will result in higher out of band linearity requirement for the receiver. To evaluate this requirement, one instance of these projected interferences from Tables 2 and 3 is further explained.

TABLE 1 The summary of the Global Positioning System receiver specifications

| Specification | Value |
|------------------------------|-------|
| Radio frequency (GHz) | 1.575 |
| Conversion gain (dB) | >90 |
| Noise figure (dB) | <6 |
| S11 (dB) | <-10 |
| Intermediate frequency (MHz) | 4 |
| P1dB (dBm) | >-30 |
| Image rejection (dB) | >25 |

TABLE 2 The summary of possible interferences in a multi-standard front-end due to IMD3

| IMD3 Interference ($2\omega_1-\omega_2$ and $2\omega_2-\omega_1$) | | | | | | | | |
|---|---------|---------|----------|----------|------------|-----------|-------------|----------|
| | GSM 850 | GSM 900 | DCS 1800 | PCS 1900 | WCDMA 2100 | 802.11b/g | Bluetooth | 802.11 a |
| GSM 850 | | | | | | - | - | - |
| GSM 900 | | | | | | - | - | - |
| DCS 1800 | | | | | | - | - | - |
| PCS 1900 | | | | | | - | - | - |
| WCDMA 2100 | | | | | | - | - | - |
| 802.11b/g | - | - | - | - | - | | - | |
| Bluetooth | - | - | - | - | - | - | | - |
| 802.11 a | - | - | GPS-BT | GPS | GPS | | GSM 850/900 | |

TABLE 3 The summary of possible interferences in a multi-standard front-end due to IMD2

| IMD2 Interference ($\omega_1-\omega_2$) | | | | | | | |
|---|---------|---------|----------|----------|------------|-----------|-----------|
| | GSM 850 | GSM 900 | DCS 1800 | PCS 1900 | WCDMA 2100 | 802.11b/g | Bluetooth |
| 802.11b/g | GPS | GPS | - | - | - | | - |
| Bluetooth | GPS | GPS | - | - | - | - | |
| 802.11 a | - | - | - | - | - | | - |

In Table 2, it can be shown that the IMD3 of BT and 802.11a standards is interfering with GSM850 band. With the help of the code written in C language, two sample channels for the BT (2450 MHz) and 802.11a (5785 MHz) are selected ($2 \times 2450 - 5785 = 850$). Also a commercial SAW filter (SAW FILTER FOR GSM850 (Rx), Murata part number: SAFEA881MFL0F00) for the calculations in the receive band is selected. The maximum power of the transmitter for BT and 802.11a are 20 and 29 dBm, respectively. The selected SAW filter introduces an attenuation of about 50 and 40 dB in the BT and 802.11a bands, respectively. About 15 dB of the antenna isolation is also considered in the calculations.¹³ Therefore, the interfering signals at the input of the GSM receiver will have an amplitude of about -45 and -26 dBm for the BT and 802.11a transmitters, respectively. The desired out-of-band IIP3 is calculated when the intermodulation signal power is 10 dB below the receiver noise floor. In a direct conversion GSM receiver, input noise level is about -121 dBm. Therefore, the IMD3 power should be less than -130 dBm and the value of necessary out of band IIP3 can be calculated as

$$IIP3 = \frac{2P_{int1} + P_{int2} - P_{IMD3in}}{2} = +7 \text{ dBm} \quad (7)$$

where in eq. 7 P_{int1} and P_{int2} are the power levels of the BT and 802.11a interferers. Thus, for the GSM receiver, out-of-band IIP3 should be higher than $+7$ dBm. These calculations for out-of-band IIP3 have been performed for other receivers in Table 2, which have intermodulation interferences occurring in their bands.

In Table 3 for the IMD2 interferences, the GPS receiver has been chosen, which has an IMD2 inside the band created by the transmitters of the GSM900 and 802.11b/g standards. If the frequency of 892 MHz from GSM band and the frequency of 2467 MHz from 802.11b/g are selected, then IMD2 tone will be equal to $2467 - 892 = 1575$ MHz, which exactly resides in the GPS band. Similar to IMD3 calculations, a commercially available SAW filter (SAW FILTER FOR GPS RF, Murata part number: SAFEB1G57FM0F00) should be considered for the investigation. The output power of GSM900 is equal to 33 dBm, whereas this value is equal to 30 dBm for the 802.11b/g standard. The selected SAW filter for the GPS band has attenuation of about 55 and 45 dB in the GSM900 and 802.11b/g bands, respectively. Again with 15-dB antenna isolation, these tones will be equal to -37 and -30 dBm for the GSM900 and 802.11b/g, respectively, at the input of the GPS receiver. In this case, the power of the IMD2 tone should be less than -120 dBm to be 10 dB below the receiver thermal noise floor. The thermal noise floor is about -108 dBm at the input of a low-IF receiver. Therefore,

the out of band IIP2 for the receiver can be calculated as

$$\text{IIP2} = P_{\text{int1}} + P_{\text{int2}} - P_{\text{IMD2in}} = +53 \quad (8)$$

Thus, the GPS receiver requires an out-of-band IIP2 larger than +53 dBm that is very challenging to achieve. Based on the requirements of out of band IIP3 and IIP2, it can be inferred that the GPS receiver has the toughest specifications among the targeted receivers. In a standalone implementation of the GPS receiver, there is no specification for the IIP2 and IIP3 of the receiver. However, in this realization of the GPS receiver, it needs to have an out-of-band IIP2 and IIP3 of about +53 and +15 dBm, respectively, to make the integration with other standards feasible.

5 | THE RECONFIGURABLE FRONT-END FOR THE MULTISTANDARD RECEIVER IN THE FREQUENCY BAND OF 800 MHz TO 2.5 GHz

The structure of the aimed multistandard receiver is shown in Figure 4. The front-end blocks have been enclosed inside a rectangular shape. The proposed front-end includes the LNA, mixer, and a TIA which has been designed as a tunable third-order low-pass filter. This TIA filter can remove part of the blocker signals and relax the specification of the final CSF in the receive chain. The requirement of the receiver in Figure 4 has been calculated with a fifth-order LPF filter. In final realization, the TIA block has a third-order filter embedded inside, which leaves about second-order of filtering for the final baseband CSF.

For instance, the proposed receiver is evaluated in GSM mode and the requirement of the blocks inside the front-end is obtained. The desired specifications for this front-end are 30 dB of gain, 3 dB of NF, and flicker noise corner frequency of about 100 kHz. The corner frequency for flicker noise is very low to attain in the CMOS process, but with the selected architecture for the receiver, it can be achieved.²⁰ The calculated IIP3 for the receiver in GSM mode is about −5 dBm. This is quite large for the entire receiver, but because a current mode architecture has been selected for the front-end, it is very promising to achieve the higher IIP3 values. In the proposed receiver (Figure 4), the front-end module includes the SAW filters and switches which can reduce the blockers and unwanted signal powers in each operation mode. However, the front-end has been realized as a wideband block and does not include any out of band filtering for the unwanted standards. Table 4 summarizes the requirements of different blocks of the receiver in the GSM mode.

5.1 | Low-noise transconductance amplifier

The proposed LNA is shown in Figure 5. This LNA is a common source amplifier with active feedback, which was introduced in Borremans et al,²¹ but later has been modified²² to perform the balun function as well. This block has been extensively discussed in Fatin and Fatin.²² In the proposed receiver, this circuit is utilized as an LNTA to be able to drive the subsequent stage that is a passive mixer designed to operate in current mode and is explained in the following section.

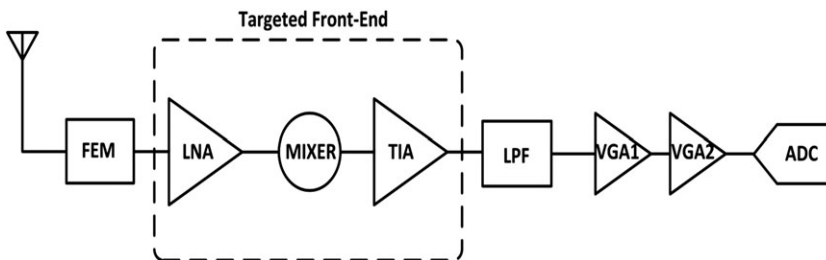


FIGURE 4 The block level implementation of the targeted front-end

TABLE 4 The requirements of different blocks of the proposed receiver in the GSM mode

| | LNA + Mixer + TIA | LPF | VGA1 | VGA2 | ADC |
|-----------------|-------------------|-----|------|------|-----|
| IIP3 (dBm) | −5 | 25 | 20 | 30 | 45 |
| NF (dB) | 4 | 20 | 20 | 20 | 20 |
| Power gain (dB) | 30 | 0 | 10 | 10 | 0 |

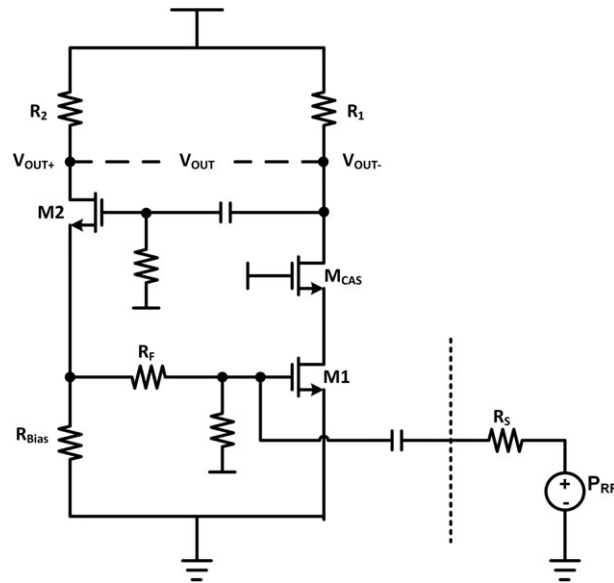


FIGURE 5 The circuit schematic of the proposed low-noise transconductance amplifier²¹

5.2 | Passive mixer

Recently, passive mixers have earned a huge interest in the structure of the radio receivers due to their better linearity and low flicker noise.²³ The passive mixer introduces loss in the conversion of the signal from RF to IF frequencies, whereas active mixer possesses the conversion gain and increases the total gain of the radio receiver. However, radio front-end does not need very high gain values, and about 30 dB of gain proves to be enough. Besides, having a front-end with moderate gain value, but with desired linearity and noise performance, then rest of the receiver gain requirement can be realized in IF stages with less power consumption and relatively easy to attain linearity and noise performance in comparison with RF frequencies.²⁴

The superiority of the passive mixer from linearity point of view is better unveiled when operating in current mode. Hence, the proposed radio front-end will operate in current mode and has architecture as shown in Figure 6. In this realization, the LNTA is taking the place of the LNA in a conventional front-end. Furthermore, in the IF section, it is necessary to have a low-impedance port facing the passive mixer over the operating bandwidth. As shown in Figure 6, this was realized by using a TIA. This TIA can be built by using an opamp inside the feedback. In this design, the proposed TIA is configured as a low-pass filter to perform part of the channel selection function as well.

The passive mixer operating in voltage mode will have a loss value of about $\pi/2$, which will increase the NF of the receiver. However, if this mixer is utilized in current mode, it can achieve the same gain value as an active mixer. The passive mixer in Figure 6 is shown without the bias voltages. However, in practice, to reduce the nonlinearity of the mixer, it should be biased near the threshold voltage. The value of this bias voltage is a trade-off between the linearity and noise of the mixer. In addition, larger transistors can improve the linearity at the expense of increase in NF of the mixer. The tail voltage of a differential pair in a Gilbert cell mixer changes its value to conduct current exactly at the zero crossing of the LO signal.²⁵ This phenomenon is not happening in the passive mixer with its terminal voltages

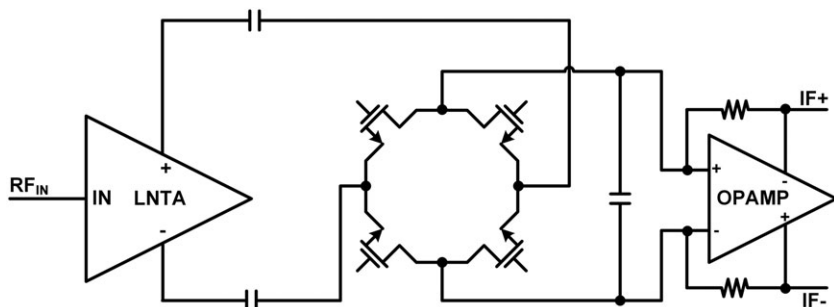


FIGURE 6 The proposed radio front-end with passive mixer

being forced by outside bias voltage into one of these three operating states: (1) OFF-overlap, (2) ON-overlap, and (3) zero-overlap. The overlap time is a period within that two transistors with same inputs have the same state and both are in on or off state. In the rest of the oscillator cycle, these transistors are in opposite states. The current mode active mixer is always operating in ON-overlap state because both transistors are ON in the transition region. The overlap state is selected based on the relative bias voltage difference between the source and gate terminals. For NMOS transistors, if $V_G < V_B + V_{th}$, then mixer is operating in OFF-overlap region. In this relation, V_G is the bias voltage of the gate terminal, V_B is the dc voltage of the IF part of the mixer, and V_{th} is equal to threshold voltage of the transistor. In this mode, it is assumed that amplitude of the oscillator signal is larger than $|V_B + V_{th} - V_G|$. If $V_G > V_B + V_{th}$, then mixer is operating in ON-overlap region. Although a voltage-mode passive mixer can operate in any of the above mentioned overlap regions, but the functionality of the current-mode mixer is better in ON-overlap region.²⁶ This is because if for part of the operation time all of the transistors will be off, then this will create a large voltage swing at the input of the mixer and take away the advantage of the current-mode operation. Although it is assumed that passive mixer does not possess flicker noise, in depth analysis shows that, with time variable drain current and even with zero mean current, MOS transistor will have noise component in DC and harmonics of the stimulating current source.²⁷ From the evaluation of the passive mixer in an architecture similar to one that is shown in Figure 6, which passive mixer is followed by a TIA, these outcomes about mixer noise can be inferred.²⁸ Despite common belief, in a passive mixer and with blockers existing in some specific frequencies of the input spectrum, the flicker noise of the switches can appear at the output of the mixer. This flicker noise value is proportional to blockers level and can be comparable with flicker noise coming from other mechanisms. In a narrow band receiver without high-frequency blockers and in a wideband receiver with small blockers, transimpedance buffer that follows the mixer determines the receiver flicker noise. If FET transistors are used to bias this buffer, their flicker noise will limit the buffer noise. Therefore, large transistors should be used in bias circuit to reduce the flicker noise. If there is some headroom for the extra voltage drop, then resistors can be used to bias the buffer and as the load elements to further remove the flicker noise sources.

In a wideband receiver, flicker noise of the switches can generate a considerable low frequency noise in the presence of the large blockers. Using an oscillator signal with sharp transitions can reduce the noise of the switches, but this will increase the power consumption of the LO buffers.

In higher frequencies, flicker noise is not dominant and the buffer noise (coming from bias circuit and load or the input transconductance) determines the receiver noise. If buffer is biased with resistors, their value should be large, although their voltage drop will limit the signal swing. If buffer is using FET transistors for biasing, their noise current should be kept as small as possible that can be achieved by small transconductance value for the transistors.

In addition to the above-mentioned points (larger transistors and biasing method), and to increase the linearity of the mixer, it should be considered that the value of the source and load impedances has strong effect on the linearity of the mixer. The source impedance of the mixer is equal to output impedance of the LNTA. It can be shown that larger output impedance for the LNTA will increase the linearity of the mixer.²⁹ The load impedance of the mixer is equal to input impedance of the TIA. This impedance should have small value not only in the bandwidth of the receiving channel but also in the out-of-band frequencies, which blocker signals exist. This will attenuate the out of band blockers as well. Otherwise, there will be large voltage swing in the terminals of the mixer that will degrade the linearity of the mixer.

As shown in Figure 6, the output signal of the LNTA is given through a coupling capacitor to the mixer. This will block flicker noise of LNTA from entering the mixer. Besides, the value of this capacitor can be set to introduce a larger impedance to $\omega_2 - \omega_1$ tone that is generated by second-order intermodulation distortion. In this state, the source impedance of the mixer at this frequency will be large and will attenuate the $\omega_2 - \omega_1$ tone; this will improve the mixer IIP2 value.

5.3 | Transimpedance amplifier

The TIA is utilized after passive mixer to create a low-impedance load over the bandwidth of the received standard. In Figure 6, this amplifier is realized by using an opamp inside feedback configuration. To have small impedance over the bandwidth, open loop gain of the opamp should be large enough and it should be maintained over the entire bandwidth of the receiver. This implicates having an opamp with large unity gain bandwidth. As mentioned before, assuming that blockers have small amplitude, the flicker and white noise of the receiver is set by noise of the TIA. The TIA noise is determined by noise of the opamp that entails designing low-noise circuits for this amplifier.

Furthermore, due to an equivalent switching impedance at the virtual ground nodes in the input of the opamp, noise of the opamp circuit can be amplified at the output of the TIA.^{27,30} This impedance is created by parasitic capacitances at the output of the LNTA. It can be observed and analyzed by using the classic switched-capacitor circuits' concept, and its value is equal to

$$R_{\text{par}} = \frac{1}{2f_{\text{LO}}C_{\text{par}}} \quad (9)$$

assuming that input referred noise of the opamp circuit is represented by $v_{n,\text{opamp}}(f)$, then the output noise will be equal to

$$v_{\text{nout,opamp}}(f) \cong \left(1 + \frac{2R_F}{R_{\text{par}}}\right) \cdot v_{n,\text{opamp}}(f) \quad (10)$$

It can be induced from eq. 10 that to increase the value of R_{par} , and assuming that frequency of the LO (f_{LO}) is fixed, parasitic tail capacitance of the mixer coming from output capacitance of the LNTA should be reduced. The larger transistors used in the mixer also increase the parasitic tail capacitance; therefore, this phenomenon also depicts the existed tradeoff between the linearity and noise of the passive mixer.

The TIA can be configured as a CSF, which can relax the requirement of the final CSF. In this realization, the TIA was designed as a second-order Butterworth filter that uses the Tow-Thomas structure and is shown in Figure 7. The Tow-Thomas structure has less sensitivity to circuit parasitics, and its corner frequency can be tuned in a simple way. The only and important change between the circuit in Figure 7 and original Tow-Thomas structure is that input resistors have been removed. This will reduce the filter noise value regarding the fact that major contribution to noise is coming from input resistors. In addition, by removal of the input resistors, the mixer circuit will face the virtual ground nodes of the opamp circuit and there will not be voltage swing at the terminals of the mixer. Because opamp has limited bandwidth and cannot maintain the low-impedance load at mixer output for high frequencies, unwanted signals for instance LO and its harmonic can create considerable voltage swings at the mixer terminals. To alleviate this issue, a capacitor is connected between the output terminals of the mixer to maintain the low-impedance port at higher frequencies and for those frequencies that are outside of the receiver bandwidth. Thus, it can attenuate the unwanted signals that are outside the receive bandwidth. This capacitor is shown in Figure 6. If this capacitor is also included inside the TIA block, then it will be equivalent to a third-order low-pass filter.

The impedance seen from input of the TIA in Figure 7 is equal to

$$Z_{\text{in}} = \frac{R_1}{(1 + sC_1R_1) \cdot [1 + A_1(s)] \cdot [1 + LG(s)]} \quad (11)$$

In this equation, R_1 and C_1 are the resistors and capacitors used in the circuit feedback loop and are shown in Figure 7. The $A_1(s)$ is the open loop gain of the first amplifier; $LG(s)$ is open loop gain of the Tow-Thomas biquad and is equal to

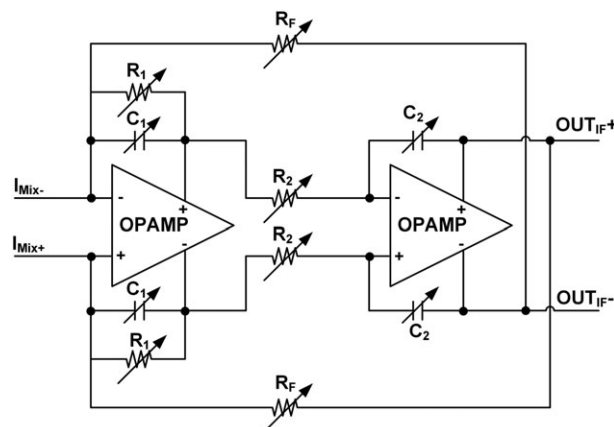


FIGURE 7 The transimpedance amplifier configured as a second-order Tow-Thomas Butterworth low-pass filter

$$LG(s) = \frac{R_1}{sR_F R_2 C_2 (1 + sC_1 R_1)} \quad (12)$$

The value of Z_{in} is very small at low frequencies, but it can increase at higher frequencies due to limited GBW of the first operational amplifier. The circuit in Figure 7 will create two complex conjugate poles that their pole and quality factor values are equal to

$$\omega_p = \frac{1}{\sqrt{R_2 R_F C_1 C_2}} \quad (13)$$

$$Q = \sqrt{\frac{R_1^2 C_1}{R_2 R_F C_2}} \quad (14)$$

To change the Q value, according to these equations, the value of R_2 resistors can be tuned, while the filter corner frequency is intact. The gain of the TIA can be altered by using the R_F resistors, whereas the bandwidth of the filter can be changed by tuning the C_1 and C_2 capacitors with the same ratio to keep the Q value unchanged.

6 | SIMULATION RESULTS

The proposed receiver has been designed, simulated, and layouted in CMOS 0.18- μm process. The proposed receiver operates in the frequency band of 800 MHz up to 2.5 GHz. This frequency band covers the most of the popular communication standards. The targeted standards mandate different IIP3 and NF values, which entail gain tunability feature in the structure of the receiver. This is realized by using a self-biased inverter that is placed between LNTA and the passive mixer (Figure 8). The front-end gain can be tuned to the desired value by changing the feedback resistors of the self-biased inverters.

The LNTA in Figure 5 is designed to provide the balanced differential output. Although higher values for R_2 can increase the gain and improve the NF, but its value cannot be increased indefinitely and should be set based on eq. 15 to create a balanced differential output signal.

$$R_2 = \left(\frac{g_{m1} R_1}{1 + g_{m1} R_1} \times \frac{1 + g_{m2} R_F}{g_{m2}} \right) \quad (15)$$

In this design, transconductance of the common source transistor (M1) in LNTA circuit is set to 60 mS to reduce the NF of the amplifier. The value of R_1 is set based on the voltage drops across the devices. The design of LNTA is based on Fatin and Fatin²² and was thoroughly explained there. The value of g_{m2} (transconductance of the M2) depends on the R_F resistor value. In this design, the R_F value is set to 280 Ω to improve the linearity of the amplifier and reduce noise of the M1 and M2 transistors. The value of R_2 was also determined based on eq. 15 and is equal to 330 Ω . As shown in Figure 5, the feedback transistor is biased through a resistor (R_{Bias}); using resistor for biasing can simplify the design

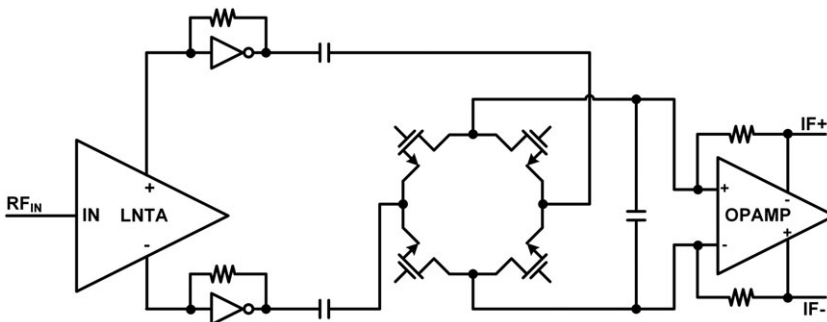


FIGURE 8 The proposed front-end with gain tunable self-biased inverters

of the input matching network. The value of this resistor is set to $800\ \Omega$ to reduce its contribution to noise of the amplifier. The passive mixer exploits large devices ($160\ \mu\text{m}/0.18\ \mu\text{m}$) and is biased in ON-overlap region. The LO signal is applied to mixer through coupling capacitor to make the independent biasing feasible. The self-biased inverters between LNTA and mixer have variable feedback resistors. The value of the capacitor that was placed between virtual ground terminals of the opamp and at the output of the mixer is equal to $5\ \text{pF}$ to eliminate the LO and its harmonics.

The operational amplifier used in TIA is shown in Figure 9. It consists of a 2-stage amplifier. Because the flicker noise of the receiver is set by the opamp circuit, the noise of the circuit should be kept as minimum as possible.³⁰ To reduce the flicker noise, the size of the input transistors is set to large value. Because the noise of the input stage determines the total noise of the opamp circuit, its transconductance is also set to higher value.

The signals at the output of the opamp can have large amplitudes especially when accompanied with unfiltered blockers; thus, the opamp supply voltage is set to $2\ \text{V}$ to increase its dynamic range. This value is still in the tolerable range of the normal transistors, and there is no need to use the high-voltage transistors of the process.

The simulation results of the opamp are shown in Figure 10. The open loop gain of the opamp is equal to $68\ \text{dB}$, and its unity gain bandwidth is at $1.15\ \text{GHz}$. The input referred noise of the amplifier is shown in Figure 11. The thermal noise of the amplifier is about $1.5\ \text{nV}/\sqrt{\text{Hz}}$, and its flicker noise corner frequency is at $700\ \text{kHz}$.

The proposed TIA is designed for two bandwidths that are 2 and $11\ \text{MHz}$. To tune the filter bandwidth, an array of binary weighted elements is used. The switches are designed as transmission gates created by NMOS and PMOS transistors.

The layout of the proposed receiver is shown in Figure 12. The area of the receiver including the bonding pads is about $2.16\ \text{mm}^2$. The simulation results of the receiver are demonstrated in the following text.

The simulation results for the input return loss (S_{11}) of the receiver are shown in Figure 13. The S_{11} value for the frequency range of $800\ \text{MHz}$ to $2.5\ \text{GHz}$ is below $-10\ \text{dB}$. The conversion gain of the radio receiver for three different gain settings and for the bandwidth of $11\ \text{MHz}$ is shown in Figure 14. This simulation demonstrates the functionality of the self-biased inverters in tuning the gain of the receiver. The conversion gain of the receiver in different operational modes and for WCDMA, WLAN, and GSM standards is shown in Figure 15. It should be mentioned that in GSM mode, the bandwidth of the TIA is set to $2\ \text{MHz}$ similar to WCDMA mode. The conversion gain of the front-end in WCDMA and WLAN modes is about $34.5\ \text{dB}$ and it is about $36\ \text{dB}$ for the GSM.

The NF of the receiver for three different aimed standards is shown in Figure 16. These simulation results indicate a minimum NF value of about $3.8\ \text{dB}$ for WLAN, $4.2\ \text{dB}$ for WCDMA, and $3.4\ \text{dB}$ for the GSM mode. The flicker noise corner frequency for WLAN is equal to $1.3\ \text{MHz}$; in WCDMA, it is about $900\ \text{kHz}$ and for GSM is about $200\ \text{kHz}$. In GSM mode, it is very crucial to have a small corner frequency for the flicker noise. Because GSM standard has small bandwidth in comparison with other standards, higher corner frequencies will require higher IF frequencies to reduce the noise corruption effect on the GSM signal. This will make the design of final CSF more difficult.

The IIP3 of the receiver in WCDMA mode is simulated by using two tones that are placed $400\ \text{kHz}$ apart. For this simulation, the frequency of LO is equal to $2.1\ \text{GHz}$. The results of this simulation are shown in Figure 17. The IIP3 of the front-end is equal to $-7\ \text{dBm}$. Excluding the GPS, the WCDMA has the toughest requirement concerning the out of band IIP3; for the in-band IIP3, its requirement is about $-17\ \text{dBm}$ for the entire receiver. This will give quite similar value for the in-band IIP3 of the front-end as in the GSM mode. As calculated before and is

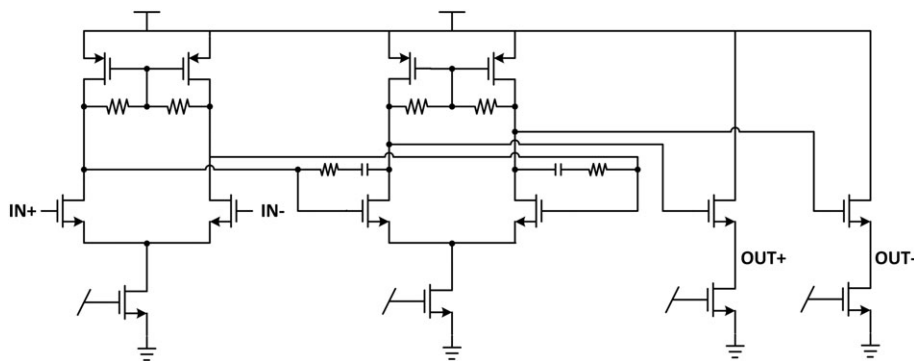


FIGURE 9 The circuit schematic of the opamp circuit used in the transimpedance amplifier

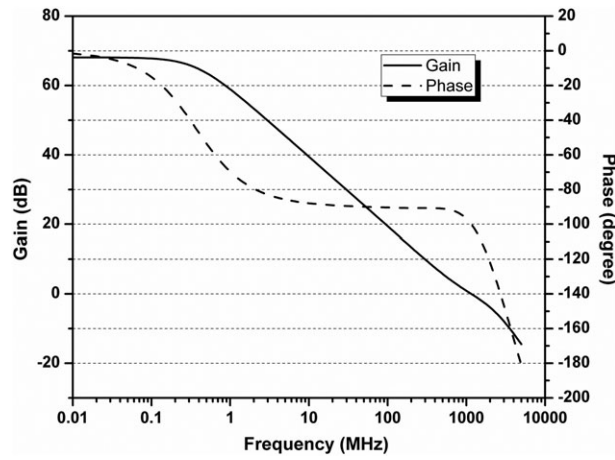


FIGURE 10 The simulation results for gain and phase of the opamp circuit used in transimpedance amplifier

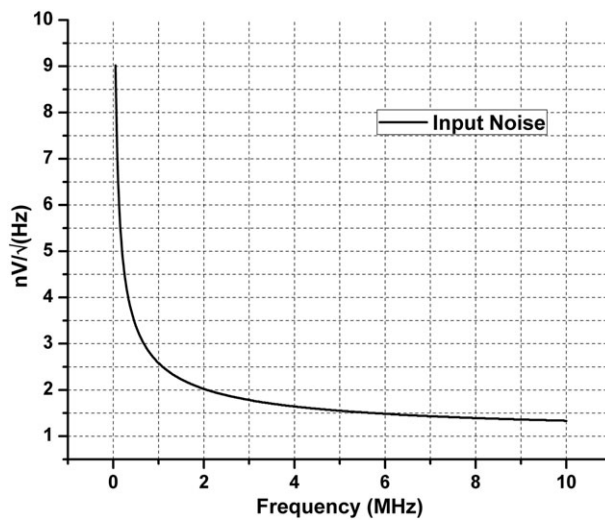


FIGURE 11 The input referred noise of the opamp circuit used in the transimpedance amplifier

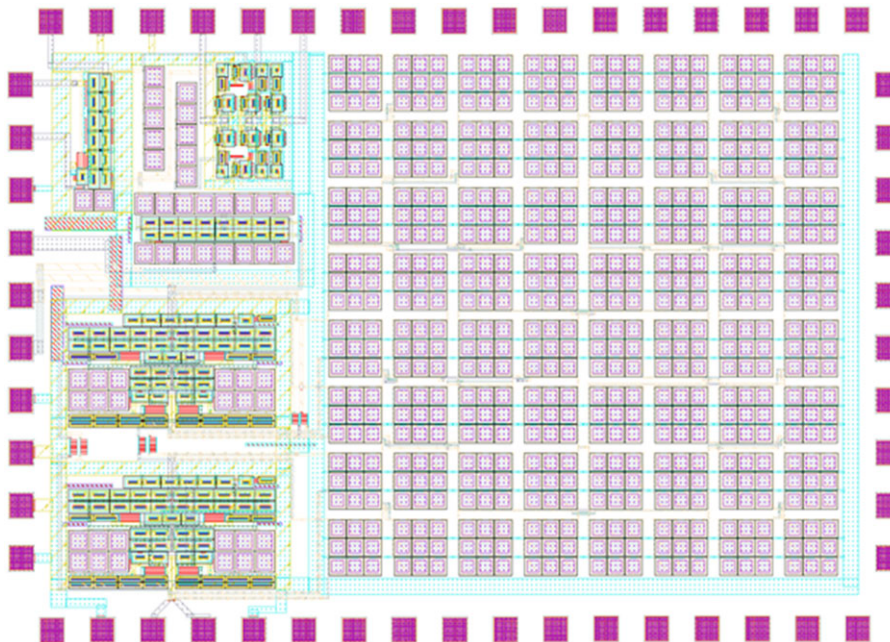


FIGURE 12 The layout of the proposed multistandard front-end [Colour figure can be viewed at wileyonlinelibrary.com]

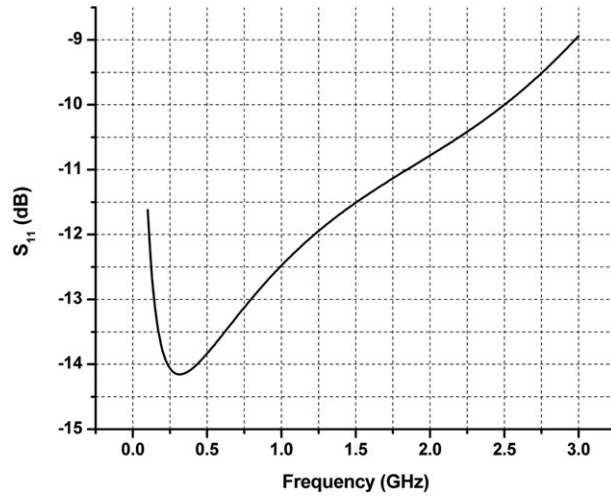


FIGURE 13 The input return loss (S_{11}) of the radio front-end

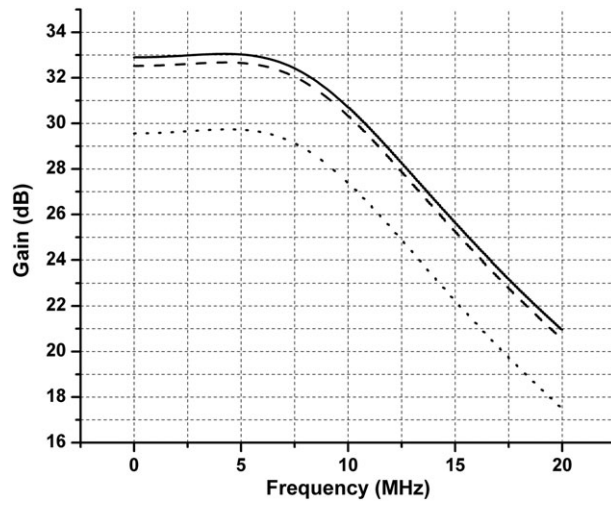


FIGURE 14 The gain tuning capability of the front-end using self-biased inverter

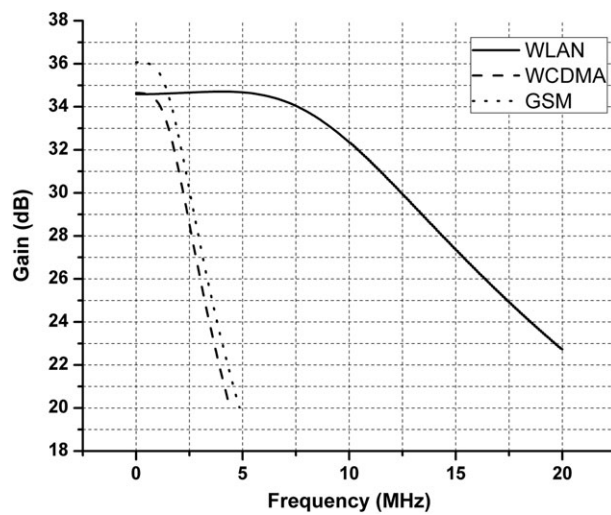


FIGURE 15 The conversion gain of the front-end for WLAN, WCDMA, and GSM standards

shown in Table 4, the required IIP3 for the front-end in GSM mode is about -5 dBm. This specified value also depends on the other blocks in the receive chain concerning their gain and linearity and will be changed in response to alterations in other blocks. However, in this design, the IIP3 of the front-end in GSM mode has been obtained based on the achievable linearity value for subsequent blocks in the receive chain. It should be pointed out here that the desired IIP3 value from system level calculations of the GSM receiver has been obtained by assuming a separate fifth-order CSF placed after the front-end. However, the value acquired in the circuit simulations comprises a third-order filtering as well. This will give the system designer extra freedom to reduce the order of the following filter and therefore make it possible to increase its IIP3 value in the system level calculations, which will relax the required IIP3 of the front-end section.

Although the noise contributions from CSF, VGAs, and ADC are not included in simulations of the front-end NF, the measured value is acceptable based on the specifications acquired from system level calculations.

Due to large bandwidth of the WLAN standards, the flicker noise corner frequency does not have considerable effect on its BER. However, in WCDMA, due to the corner frequency of about 900 kHz and its smaller bandwidth in comparison with WLAN, the flicker noise effect on its BER should be evaluated.

In GSM mode, the low-IF architecture seems reasonable where IF filtering can be done in analog domain. However, limited dynamic range of the active analog filter,^{31,32} which is more severe in bandpass state, will hinder this realization. In this implementation and for GSM standard, the low-IF architecture with IF frequency of about 400 kHz seems more feasible. In this state, the blocker signals first will be mostly filtered out in analog domain by using a low-pass filter with bandwidth of 500 kHz. Then, bandpass filtering at IF frequency of 400 kHz can be deferred to digital domain, which can be performed in a way that can resemble an ideal filtering.

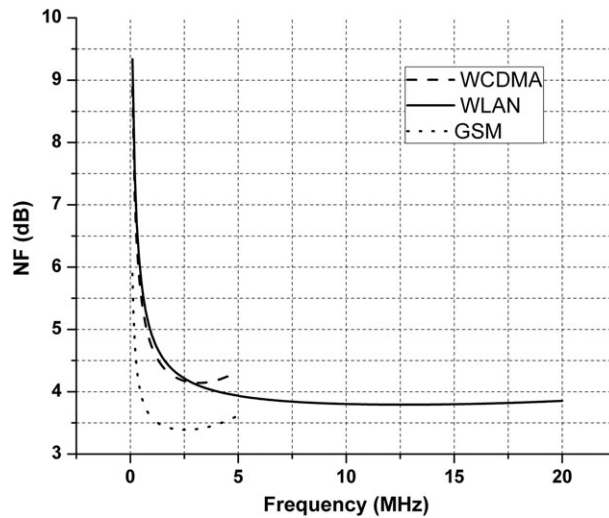


FIGURE 16 The noise figure of the front-end in different operational standards

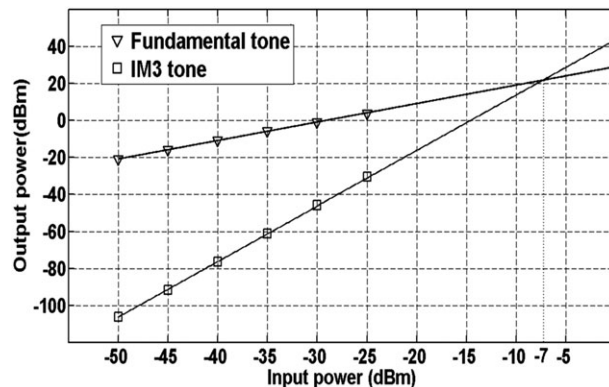


FIGURE 17 The IIP3 of the front-end in WCDMA mode

The simulated IIP2 of the receiver is shown in Figure 18. The IIP2 is equal to +66 dBm. The simulated IIP2 demonstrates the receiver resilience to tones generated by second-order nonlinearity. Although the more realistic simulation needs to account for devices mismatches and changes which needs to include the Monte Carlo simulation along with this test; however, the results obtained from the simulation are still very promising for the entire front-end.

Although the reported results for the front-end have been obtained from careful simulations, it should be mentioned that to get absolutely accurate and reliable results and to entirely evaluate the proposed design, the measurement of the final fabricated chip would be necessary. In this case, for instance, by doing measurement on several samples of the fabricated chip, the distribution of the IIP2 will be measured and the effect of the different mismatch sources on the IIP2 value will be figured out to a great extent. This explanation is also true for power consumption and other specifications such as IIP3, which can be differed from their simulation value.

The power consumption of the front-end is about 78 mW. This power consumption includes the power consumption of the LNTA, mixer, and TIA. The TIA power is consumed inside two operational amplifiers. The passive mixer does not have static bias current.

The LNTA consumes 21.6 mW from total power consumption, whereas self-biased inverters and TIA consume about 8.64 and 47.5 mW, respectively. Figure 19 shows the distribution of the power consumption over the different building blocks of the front-end. According to this chart, the RF segment (LNTA + mixer) consumes about 39% of the total power, while the TIA uses up most of the remaining power.

The out-of-band IIP3 in GPS mode is measured by using two tones at 1.862 GHz representing the PCS and the other at 5.3 GHz for the IEEE 802.11a. The power of these tones are equal to -35 and -21 dBm, respectively, which are set based on the system level calculations. The IMD3 of these tones lies in the GPS band. The power of this IMD3 tone is about -102 dBm and is shown in Figure 20. Then, based on the power of the IMD3 and input tones, the out-of-band IIP3 can be calculated as in eq. 16,

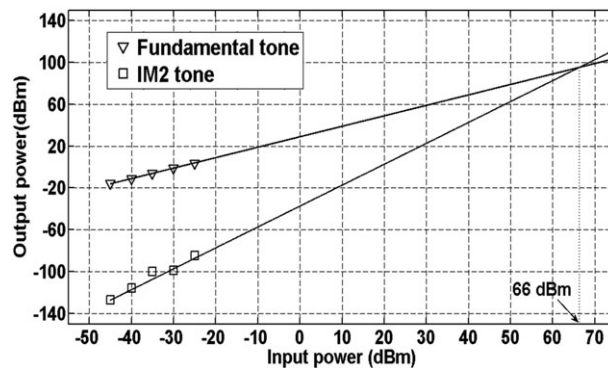


FIGURE 18 The IIP2 of the front-end in WCDMA mode

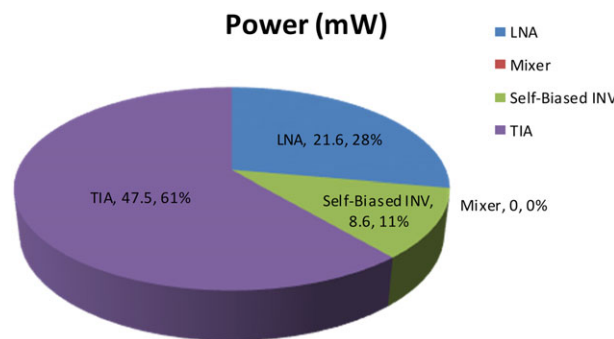


FIGURE 19 The distribution of the power consumption over different building blocks of the front-end [Colour figure can be viewed at wileyonlinelibrary.com]

$$P_{\text{IIP3O}} = \frac{2P_{\text{PCS}} + P_{\text{WLAN}} - P_{\text{IMD3}}}{2} = +5.5 \text{ dBm} \quad (16)$$

This achieved value for the out of band IIP3 is less than targeted value of +15 dBm. One remedy for improvement of this out of band IIP3 is to use wideband resonators that can be placed at output of the LNTA or after self-biased inverters.

The out-of-band IIP2 in GPS mode was investigated by using two tones at 892 MHz (GSM900) and the other at 2.467 GHz (802.11b/g or BT). The power of these tones are about -37 and -30 dBm, respectively. As shown in Figure 21, the generated IMD2 tone resides in GPS band, and its power is about -81 dBm. Therefore, the out-of-band IIP2 is calculated as in eq. 17,

$$P_{\text{IIP2O}} = P_{\text{GSM}} + P_{\text{WLAN}} - P_{\text{IMD2}} = +14 \text{ dBm} \quad (17)$$

This value is much smaller than desired +53 dBm, which indicates that implementation of the GPS receiver in a wideband receiver and along with other standards is very challenging. This would lead to narrow band realization for the GPS receiver, which can use on-chip narrowband resonators and off-chip matching networks to get a desirable filtering of unwanted tones coming from other standards.

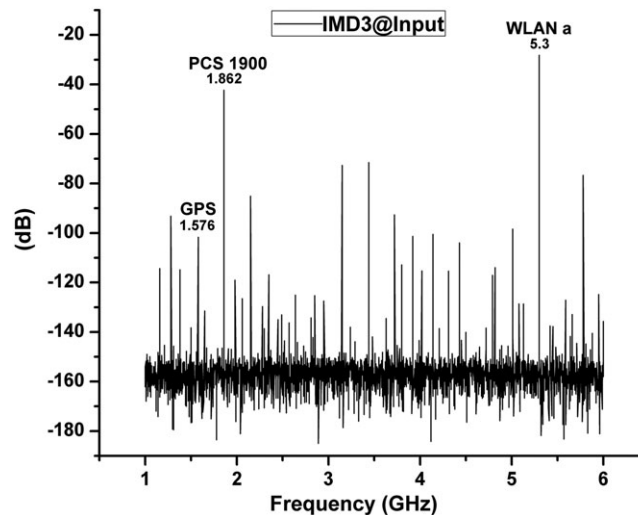


FIGURE 20 The out of band IIP3 of the front-end in Global Positioning System mode

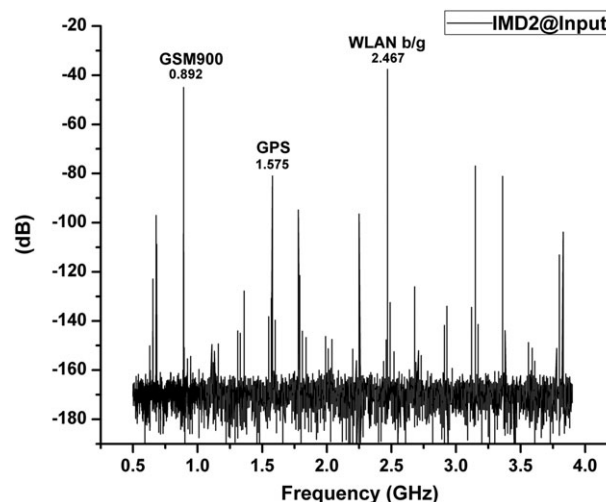


FIGURE 21 The out of band IIP2 of the front-end in Global Positioning System mode

TABLE 5 Simulation summary and comparison of the proposed multistandard front-end with two recently reported works

| Parameter | This Work | 29 | 30 |
|--------------------------|--------------------|--------------------|-----------------|
| RF operation band (GHz) | 0.8-2.5 | 0.6-3 | 0.17-1.7 |
| Maximum gain (dB) | 36 ^a | 48 | 35 |
| NF (dB) | 3.4 ^a | 3 | 4 |
| IIP3 (dBm) | -7 ^b | -14 | -3.4 |
| IIP3 (out of band) (dBm) | +5.5 | NA | NA |
| IIP2 (dBm) | +66 ^b | NA | +32 |
| IIP2 (out of band) (dBm) | +14 | NA | NA |
| S11 (dB) | <-10 | <-8 | <-10 |
| Power (mW) | 78 | 30 | 55 |
| Supply (V) | 1.8 | 1.2 | 1.2 |
| Process CMOS | 0.18 μm | 0.13 μm | 65 nm |
| Baseband filter order | 3rd | 3rd | 3 rd |
| Area (mm ²) | 2.16 | 1.5 | 0.46 |

^aGSM mode.^bWCDMA mode.

Table 5 summarizes and compares the simulation results of the proposed front-end with two recently reported designs.^{33,34} Although the results of the proposed design are obtained from simulations, the simulations have been carried out with great accuracy and including the every detail to closely resemble the measurement results.

7 | CONCLUSIONS

In this paper, a reconfigurable front-end for the reception of the standards residing in the frequency range of 800 MHz to 2.5 GHz is proposed. The realization is in wideband form and targets the GSM, WCDMA, and WLAN b/g standards. Because GPS signal also resides in this frequency range, its realization along with other standards was investigated. The most challenging specification for implementation of the GPS receiver in this scenario is out of band linearity. The simulation results of the implementation for different aimed standards are close to the required specifications based on the system level calculations. However, out-of-band linearity simulations for the GPS came short of fulfilling the desired specifications that will lead to and suggest the narrowband implementation for the GPS band. This will require a separate implementation for the GPS receiver in a single-mode narrow-band state.

ORCID

G. Zare Fatin  <http://orcid.org/0000-0001-6346-5460>

Jafar Sobhi  <http://orcid.org/0000-0002-8109-9182>

REFERENCES

- Shi Z, Salminen O, Hsu K, et al. "A 2.7-V mixed signal processor for CDMA/AMPS cellular phones," *IEEE RFIC Digest of Papers*. June 1999;29-32.
- Fong KL. "Dual-band high-linearity variable-gain low-noise amplifiers for wireless applications," *IEEE ISSCC Digest of Technical Papers*. Feb. 1999;224-225.
- Abidi AA. The path to the software-defined radio receiver. *IEEE ISSCC Digest of Technical Papers*. May 2007;42(5):954-966.
- Molnar A, Magoon R, Hatcher G, et al. "A single-chip quad-band (850/900/1800/1900 MHz) direct-conversion GSM/GPRS RF transceiver with integrated VCOs and fractional-N synthesizer," *IEEE ISSCC Digest of Technical Papers*. Feb. 2002;232-233.
- Duvivier E, Puccio G, Cipriani S, et al. A fully integrated zero-IF transceiver for GSM-GPRS quad-band application. *IEEE J Solid State Circuits*. Dec. 2003;38(12):2249-2257.

6. Cipriani S., et al. "Fully integrated zero IF transceiver for GPRS/GSM/DCS/PCS applications," Proceeding of ESSCIRC. Sep. 2002;439–442.
7. Quinlan P, Crowley P, Chanca M, et al. "A multi-mode 0.3–128 kb/s transceiver for the 433/868/915 MHz ISM bands in 0.25 μm CMOS," IEEE ISSCC Digest of Technical Papers. Feb. 2004;274–275.
8. Götz E., Kröbel H, Märzinger G, et al. "A quad-band low power single chip direct conversion CMOS transceiver with $\Sigma\Delta$ -modulation loop for GSM," Proceedings ESSCIRC. Sep. 2003;217–220.
9. Agnelli F, Albasini G, Bietti I, et al. Wireless multi-standard terminals: system analysis and design of a reconfigurable RF front-end. *IEEE Circuits Syst Mag.* 2006;6(issue 1):38–59, First Quarter.
10. Tasic A, Serdijn WA, Long JR. Adaptive multi-standard circuits and systems for wireless communications. *IEEE Circuits Syst Mag.* 2006;6(1):29–37, First Quarter.
11. Pärssinen A. System design for multi-standard radios. In: *IEEE ISSCC Conf. Dig. Tech. Papers*; 2006:5–9.
12. Zare Fatin G, Koozehkanani ZD, Sjöland H. A 90 nm CMOS +11 dBm IIP3 4 mW dual-band LNA for cellular handsets. *IEEE Microwave Wireless Compon Lett.* Sep. 2010;20(9):513–515.
13. Gustafsson M, Prssinen A, Bjorkstn P, et al. A low noise figure 1.2-V CMOS GPS receiver integrated as a part of a multimode receiver. *IEEE J Solid State Circuits.* July 2007;42(7):1492–1500.
14. Fatin GZ, Osgooei MS, Fotowat-Ahmady A. I/Q mismatch calibration of a transmitter using local quadrature oscillator. *Microchem J.* September 2016;55:82–91.
15. ETSI TS 100 910 V8.6.0 (2000–09), "Digital cellular telecommunications system (phase 2+); radio transmission and reception (3GPP TS 05.05 version 8.6.0 Release 1999)," Technical Specification.
16. Jensen OK, Kolding TE, Iversen CR, et al. RF receiver requirements for 3G W-CDMA mobile equipment. *Microw J.* Feb. 2000;43(2):22–46.
17. Gatta F, Manstretta D, Rossi P, Svelto F. A fully integrated 0.18- μm CMOS direct conversion receiver front-end with on-chip LO for UMTS. *IEEE J Solid State Circuits.* Jan. 2004;39(1):15–23.
18. Rogin J, Kouchev I, Brenna G, Tschopp D, Qiuting Huang. A 1.5-V 45-mW direct-conversion WCDMA receiver IC in 0.13- μm CMOS. *IEEE J Solid State Circuits.* Dec. 2003;38(12):2239–2248.
19. Behzad A. *Wireless LAN Radios, System Definition to Transistor Design.* IEEE Press; 2008.
20. Sacchi E, et al. "A 15 mW, 70 kHz 1/f corner direct conversion CMOS receiver," Proceedings of the IEEE Custom Integrated Circuits Conference. 2003;459–462.
21. Borremans J, Wambacq P, Soens C, Rolain Y, Kuijk M. Low-area active-feedback low-noise amplifier design in scaled digital CMOS. *IEEE J Solid State Circuits.* Nov. 2008;43(11):2422–2433.
22. Fatin GZ, Fatin HZ. A wideband Balun-LNA. *AEU-Int J Electron C.* July 2014;68(7):653–657.
23. Kaczman D, Shah M, Alam M, et al. A single-chip 10-band WCDMA/HSDPA 4-band GSM/EDGE SAW-less CMOS receiver with DigRF 3G interface and 90 dBm IIP2. *IEEE J Solid State Circuits.* March 2009;44(3):718–739.
24. Blaakmeer SC, Klumperink EAM, Leenaerts DMW, Nauta B. Wideband Balun-LNA with simultaneous output balancing, noise-canceling and distortion-canceling. *IEEE J Solid State Circuits.* June 2008;43(6):1341–1350.
25. Zareh Fatin GH, Savadi Oskooei M, Koozeh Kanani ZD. A technique to improve noise figure and conversion gain of CMOS mixers. In: *50th Midwest Symposium on Circuits and Systems, MWSCAS*; 2007.
26. Chehrazi S, Bagheri R, Abidi AA, "Noise in passive FET mixers: a simple physical model," Proceedings of the IEEE Custom Integrated Circuits Conference. Oct. 2004;375–378.
27. Redman-White W, Leenaerts DMW, "1/f noise in passive CMOS mixers for low and zero IF integrated receivers," Proceedings of the 27th European Solid-State Circuits Conference, ESSCIRC. Sept. 2001;2001:41–44.
28. Chehrazi S, Mirzaei A, Abidi AA. Noise in current-commutating passive FET mixers. *IEEE Trans Circuits Syst Regul Pap.* Feb. 2010;57(2):332–344.
29. Khatri H, Gudem PS, Larson LE. Distortion in current commutating passive CMOS downconversion mixers. *IEEE Trans Microwave Theory Tech.* Nov. 2009;57(11):2671–2681.
30. Valla M, Montagna G, Castello R, Tonietto R, Bietti I. A 72-mW CMOS 802.11a direct conversion front-end with 3.5-dB NF and 200-kHz 1/f noise corner. *IEEE J Solid State Circuits.* April 2005;40(4):970–977.
31. Zareh Fatin GH, Ghadami M. A very low power 10 MHz CMOS continuous-time bandpass filter with on-chip automatic tuning. *IEICE Trans Electron.* July 2006;E89-C(7):1089–1096.
32. Zareh Fatin G, Koozeh Kanani ZD. A very low power bandpass filter for low-IF applications. *J Circuit, Syst Comput.* Aug. 2008;17(4).
33. Wang X, Sturm J, Yan N, Tan X, Min H. 0.6–3-GHz wideband receiver RF front-end with a feedforward noise and distortion cancellation resistive-feedback LNA. *IEEE Trans Microwave Theory Tech.* Feb. 2012;60(2):387–392.

34. Mak P-I, Martins RP. A 0.46-mm² 4-dB NF unified receiver front-end for full-band mobile TV in 65-nm CMOS. *IEEE J Solid State Circuits*. Sep. 2011;46(9):1970-1984.

How to cite this article: Zare Fatin G, Koozehkanani ZD, Fotowat-Ahmady A, Sobhi J, Farrell R. Design of a reconfigurable front-end for a multistandard receiver for the frequency range of 800 MHz to 2.5 GHz. *Int J Circ Theor Appl*. 2018;46:1144–1165. <https://doi.org/10.1002/cta.2476>